www.sciencemag.org/345/6200/1027/suppl/DC1

Supplementary Materials for

Observation of the transition state for pressure-induced $BO_3 \rightarrow BO_4$ conversion in glass

Trenton Edwards, Takatsugu Endo, Jeffrey H. Walton, Sabyasachi Sen*

*Corresponding author. E-mail: sbsen@ucdavis.edu

Published 29 August 2014, *Science* **345**, 1027 (2014)
DOI: 10.1126/science.1256224

This PDF file includes:

Supplementary Materials:

Materials and Methods

The borosilicate glass Corning code 7059 was chosen for the present study. This glass has a chemical composition of (mol%) 12.5% BaO, 8.5% Al_2O_3, 16% B_2O_3, and 63% SiO_2 and a calorimetric glass transition temperature T_g of ~ 950 K *(18)*. Drawn sheets (150.0 x 150.0 x 1.1 mm) of this glass were obtained from Corning Incorporated. Samples were core drilled from a glass sheet to obtain rods of ~ 1 mm diameter by 3 mm length for high-pressure studies. The *in situ* high-pressure ^{11}B wideline NMR spectroscopic measurements were carried out using a home-built high-pressure NMR probe (see below, for details) in a horizontal bore (bore inner diameter 180 mm) 7T Bruker imaging magnet equipped with a Bruker BioSpec spectrometer system operating at a ^{11}B Larmor frequency of 96 MHz. Single-pulse ^{11}B NMR spectra were collected at various pressures ranging between ambient and 2 GPa, using a $\pi/8$ solids pulse (0.4μs) with a recycle delay of 1 s. Approximately 10,000 free induction decays were averaged and Fourier transformed to obtain each spectrum.

Two samples core drilled from the same glass sheet were subjected to high P-T conditions in a 6-8 multi anvil apparatus for *ex situ* high-resolution ^{11}B magic-angle-spinning (MAS) NMR spectroscopic measurements. One of the samples was taken to 8 GPa at ambient temperature and equilibrated for 12 hours before decompression at a rate of 4 GPa/h. Another sample was taken to 2 GPa and subsequently heated to 1000 K, equilibrated at that temperature for 2 hours followed by thermal quenching at 50 K/s and subsequently decompression at 4 GPa/h. ^{11}B MAS NMR spectra of these two samples and of the as-received glass were collected using a 11.7T magnet (Bruker) and a spectrometer (Bruker Avance500) operating at a ^{11}B

Larmor frequency of 160.4 MHz. Single-pulse ^{11}B NMR spectra were collected using a MAS probe (Doty Inc.) with a $\pi/10$ solids pulse (0.25μs) and a recycle delay of 0.25 s. Crushed samples were taken in a ZrO_2 rotor and were spun at 12 kHz. Approximately 3000 to 12000 free induction decays were averaged and Fourier transformed to obtain each spectrum.

Table S1.^{11}B NMR parameters for BO_3 and BO_4 sites obtained from simulation of the ^{11}B wideline NMR spectra obtained *in situ* at various pressures.

Pressure	**Coordination Environment**	**C_Q (MHz) (±0.05)**	**η**	**δ_{iso} (ppm)**	**FWHM (ppm)**	**Relative fraction (±2%)***
0.1 MPa	BO_3	2.70	0.0	17.3	–	75
	BO_4	~ 0.00	–	0.5	32.5	25
1.0 GPa	BO_3	2.73	0.0	19.0	–	75
	BO_4	~ 0.00	–	0.4	33.0	25
1.6 GPa	BO_3	2.73	0.0	19.9	–	76
	BO_4	~ 0.00	–	0.4	34.5	24
2.0 GPa	BO_3	2.75	0.0	20.6	–	75
	BO_4	~ 0.00	–	0.5	31.4	25

*Relative error between spectra

Table S2. ^{11}B NMR parameters for BO_3 and BO_4 sites obtained from simulation of the ^{11}B MAS NMR spectra.

Sample	**Coordination Environment**	**C_Q (MHz) (±0.05)**	**η**	**δ_{iso} (ppm)**	**FWHM (ppm)**	**Relative fraction (±1%)***
As-received glass	BO_3	2.60	0.0	16.2	–	76
	BO_4	~ 0.00	–	0.5	2.9	24
Quenched from 2 GPa and 1000K	BO_3	2.67	0.0	15.9	–	70
	BO_4	~ 0.00	–	–0.3	3.3	30
Quenched from 8 GPa and 298 K	BO_3	2.70	0.0	16.4	–	74
	BO_4	~ 0.00	–	0.3	3.0	26

*Relative error between spectra

High-pressure NMR Probe

The *in situ* high-pressure NMR experiments were carried out using a custom-built NMR probe where the glass sample was pressurized using a cylindrical high-pressure cell (*EasyCell 30*, Almax-Easylab) that was configured for NMR measurements *(19)*. A simple cross-sectional schematic of the cell configuration is shown in Fig. S1. The cell sleeve consists of an outer and an inner shell made of non-magnetic Cu-Be alloy and MP35N superalloy, respectively *(20)*. The 7059 glass plate was core drilled to obtain rods ~ 1 mm diameter by 3 mm length and an NMR coil was then fitted around the sample rod and the leads were epoxied into a pressure cell feed-through (Figs. S1,S2). The sample/coil is fitted inside a Teflon® cylindrical cup filled with Daphne 7373 paraffin industrial oil as a pressure transmitting fluid and is held in the pressure sleeve using a locking nut *(21)*. Pressure is applied to the Teflon cup using a hydraulic ram traveling through a hollow locking nut and subsequently advancing a sapphire piston (8mm diameter x 25mm length) from the opposite end of the cell. The piston-side locking nut secures the advancing piston, allowing for the cell to remain pressurized when separated from the hydraulic press. The compression of the Teflon cap and fluid allow for the application of hydrostatic pressure on the sample. Cell pressure was determined from the applied hydraulic pressure that was calibrated in separate runs using known pressure dependence of the electrical resistance of a manganin wire *(22)*. The loaded pressure cell is placed in the NMR probe (Fig. S2) and positioned such that the coil is perpendicular to the applied external magnetic field.

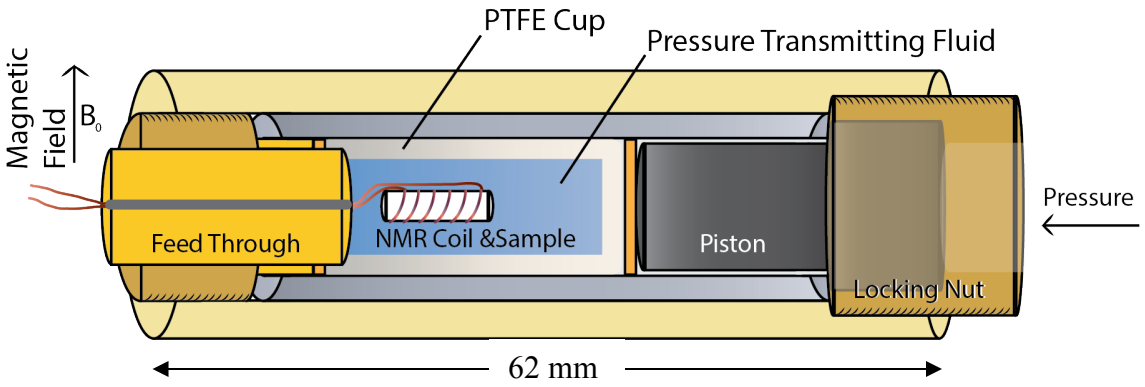

Figure S1.Pressure cell schematic. External pressure is applied to advance a piston and compress a PTFE cup containing a pressure transmitting fluid. A sample suspended in the fluid experiences hydrostatic pressure and a custom NMR coil placed around the sample allow for in-situ HP-NMR experiments. All component materials are chosen such that the pressurizing cell is completely non-magnetic. **Cell components shown are not to scale.*

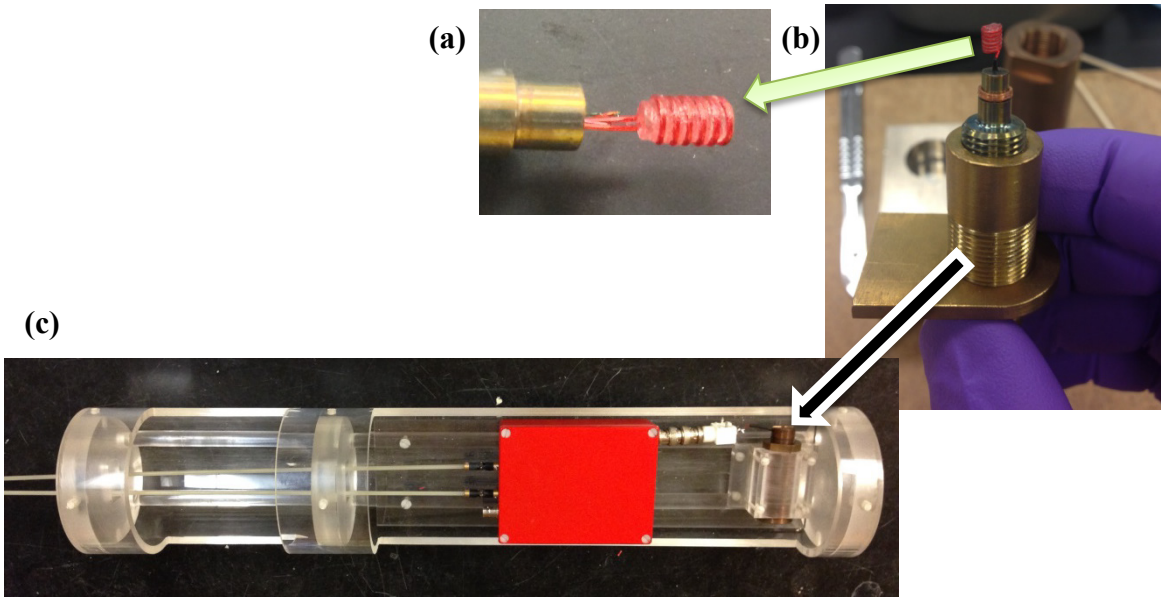

Figure S2. a) Sample glass rod fitted with a coil,(b) epoxied into the high pressure feed-through of the pressure cell and (c) loaded cell fitted to home-built NMR probe

***Ex situ* experiments in Multi-anvil cell**

In the case of the multi-anvil cell experiments, glass samples were taken in graphite capsulewithin an 8 mm truncated edge length castable MgO ceramic octahedron. The capsule also served as a resistance heater for high temperature experiment wherethe sample temperature was monitored by a Type D (W3%Re - W25%Re) thermocouple and pressure was determined using fixed-point pressure standards based on phase transitions in crystalline Bi and ZnTe.

***Ab initio* calculations of ^{11}B NMR parameters**

Ab initio calculations of ^{11}B NMR parameters were carried out on a molecule of H_3BO_3, as a function of systematic changes in the position of the central B atom, using density functional theory (DFT) within the Gaussian 09 program package *(23)*. The 6-311+G(d,p) basis sets based on Becke's three-parameter hybrid method with the LYP correlation (B3LYP) were used *(24,25)*. The corresponding ^{11}B NMR parameters were computed using the continuous set of gauge transformations (CSGT) method *(26-28)*. The experimental ^{11}B isotropic chemical shift δ_{iso} = 19.6 ppm was used as reference for the fully optimized structure of the H_3BO_3 molecule.

The effects of three types of deformation of the B coordination geometry on the ^{11}B NMR parameters are considered. In the case of **Model 1**, a uniform compression/expansion of the B-O coordination triangle is considered (Fig. S3). The corresponding ^{11}B NMR parameters for the H_3BO_3 molecule as a function of B-O bond length are listed in Table S3.

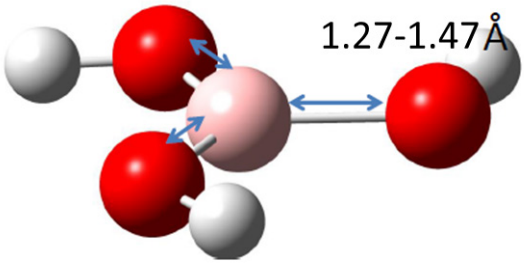

Figure S3. Uniform compression/expansion of BO_3 triangle in Model 1.

Table S3. Calculated ^{11}B NMR parameters for the H_3BO_3 molecule as a function of B-O bond length, upon deformation according to Model 1.

B-O bond length (Å)	**C_Q (MHz)**	**η**	**δ_{iso} (ppm)**
1.27	2.49	0.0	12.9
1.32	2.48	0.0	17.3
1.37*	2.49	0.0	19.6
1.42	2.49	0.0	24.7
1.47	2.45	0.0	28.2

* *Fully optimized equilibrium (undeformed) structure*

In the case of **Model 2**, the BO_3 environment was deformed in an anisotropic fashion where one of the B-O distances was systematically increased from 1.37 to 1.47Å while the other two distances were allowed to relax within the B-O plane to a minimum energy configuration. (Fig. S4). The corresponding ^{11}B NMR parameters for the H_3BO_3 molecule as a function of the unique B-O bond length are listed in Table S4.

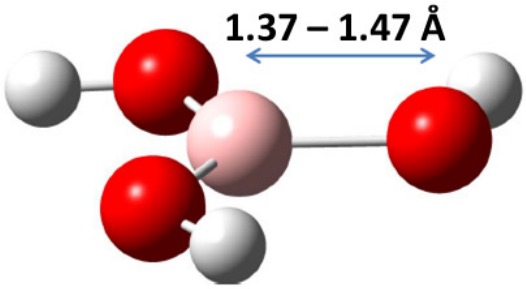

Figure S4. In-plane displacement of the B atom according to Model 2.

Table S4. Calculated ^{11}B NMR parameters for the H_3BO_3 molecule as a function of the unique (long) B-O bond length, upon deformation according to Model 2.

B-O bond length (Å)	**C_Q (MHz)**	**η**	**δ_{iso} (ppm)**
1.37*	2.49	0.0	19.6
1.42	2.48	0.0	20.6
1.47	2.45	0.0	21.5

* *Fully optimized equilibrium (undeformed) structure*

In the case of **Model 3**, the central B atom is moved vertically out of the plane of the oxygen atoms along the threefold symmetry axis and all three B-O distances were allowed to relax (Fig. S5). The corresponding ^{11}B NMR parameters for the H_3BO_3 molecule as a function of the vertical distance of the B atom from the oxygen plane and of the average B-O bond length are listed in Table S5.

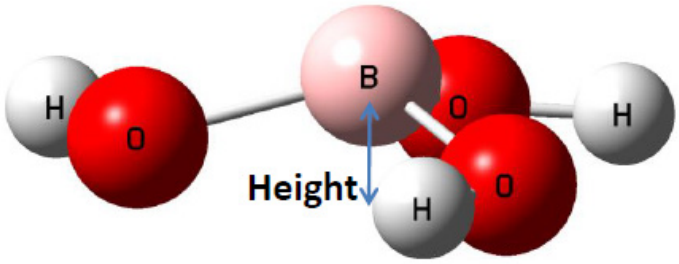

Figure S5. Vertical displacement of the B atom from the oxygen plane along the C_3 axis, in Model 3.

Table S5. Calculated ^{11}B NMR parameters for the H_3BO_3 molecule upon deformation according to Model 3.

Vertical height of B above O_3 plane (Å)	**B-O bond length (Å)**	**C_Q (MHz)**	**η**	**δ_{iso} (ppm)**
0.000*	1.370	2.49	0.0	19.6
0.196	1.374	2.47	0.0	20.4
0.279	1.379	2.44	0.0	21.4
0.345	1.385	2.43	0.0	22.6

* *Fully optimized equilibrium (undeformed) structure*

References and Notes

1. S. R. Elliott, *The Physics and Chemistry of Solids* (Wiley, New York, ed. 1, 1998).

2. G. N. Greaves, S. Sen, Inorganic glasses, glass-forming liquids and amorphizing solids. *Adv. Phys.* **56**, 1–166 (2007). doi:10.1080/00018730601147426

3. G. H. Wolf, P. F. McMillan, in *Structure, Dynamics and Properties of Silicate Melts*, J. F. Stebbins, P. F. McMillan, D. B. Dingwell, Eds., Reviews in Mineralogy, vol. 32 (Mineralogical Society of America, Washington, DC, 1995).

4. J. F. Stebbins, NMR evidence for five-coordinated silicon in a silicate glass at atmospheric pressure. *Nature* **351**, 638–639 (1991). doi:10.1038/351638a0

5. S. Sen, Z. Xu, J. F. Stebbins, Temperature dependent structural changes in borate, borosilicate and boroaluminate liquids: High-resolution 11B, 29Si and 27Al NMR studies. *J. Non-Cryst. Solids* **226**, 29–40 (1998). doi:10.1016/S0022-3093(97)00491-2

6. S. Sen, Temperature induced structural changes and transport mechanisms in borate, borosilicate and boroaluminate liquids: High-resolution and high-temperature NMR results. *J. Non-Cryst. Solids* **253**, 84–94 (1999). doi:10.1016/S0022-3093(99)00346-4

7. S. Sen, T. Topping, P. Yu, R. E. Youngman, Atomic-scale understanding of structural relaxation in simple and complex borosilicate glasses. *Phys. Rev. B* **75**, 094203 (2007). doi:10.1103/PhysRevB.75.094203

8. S. S. Uzun, S. Sen, ^{11}B MAS NMR spectroscopic study of structural relaxation, aging, and memory effect at the atomic scale in a borosilicate glass. *J. Phys. Chem. B* **111**, 9758–9761 (2007). Medline doi:10.1021/jp072223i

9. L. Wondraczek, S. Sen, H. Behrens, R. E. Youngman, Structure-energy map of alkali borosilicate glasses: Effects of pressure and temperature. *Phys. Rev. B* **76**, 014202 (2007). doi:10.1103/PhysRevB.76.014202

10. F. Angeli, O. Villain, S. Schuller, T. Charpentier, D. de Ligny, L. Bressel, L. Wondraczek, Effect of temperature and thermal history on borosilicate glass structure. *Phys. Rev. B* **85**, 054110 (2012). doi:10.1103/PhysRevB.85.054110

11. F. Michel, L. Cormier, P. Lombard, B. Beuneu, L. Galoisy, G. Calas, Mechanisms of boron coordination change between borosilicate glasses and melts. *J. Non-Cryst. Solids* **379**, 169–176 (2013). doi:10.1016/j.jnoncrysol.2013.08.007

12. L.-S. Du, J. R. Allwardt, B. C. Schmidt, J. F. Stebbins, Pressure-induced structural changes in a borosilicate glass-forming liquid: Boron coordination, non-bridging oxygens, and network ordering. *J. Non-Cryst. Solids* **337**, 196–200 (2004). doi:10.1016/j.jnoncrysol.2004.03.115

13. Materials and methods are available as supplementary materials on *Science* Online.

14. G. L. Turner, K. A. Smith, R. J. Kirkpatrick, E. Oldfield, *J. Magn. Reson.* **67**, 544–550 (1986).

15. S. Kroeker, J. F. Stebbins, Three-coordinated boron-11 chemical shifts in borates. *Inorg. Chem.* **40**, 6239–6246 (2001). Medline doi:10.1021/ic010305u

16. S. Sen, Density functional theory calculations of ^{11}B NMR parameters in crystalline borates. *Mol. Simul.* **34**, 1115–1120 (2008). doi:10.1080/08927020802258716

17. M. Guignard, L. Albrecht, J. W. Zwanziger, Zero-stress optic glass without lead. *Chem. Mater.* **19**, 286–290 (2007). doi:10.1021/cm062208a

18. J. C. Mauro, S. S. Uzun, W. Bras, S. Sen, Nonmonotonic evolution of density fluctuations during glass relaxation. *Phys. Rev. Lett.* **102**, 155506 (2009). Medline doi:10.1103/PhysRevLett.102.155506

19. X. F. Wang, R. H. Liu, Z. Gui, Y. L. Xie, Y. J. Yan, J. J. Ying, X. G. Luo, X. H. Chen, Superconductivity at 5 K in alkali-metal-doped phenanthrene. *Nat. Commun.* **2**, 507 (2011).doi:10.1038/ncomms1513 Medline

20. I. R. Walker, Nonmagnetic piston–cylinder pressure cell for use at 35 kbar and above. *Rev. Sci. Instrum.* **70**, 3402–3412 (1999). doi:10.1063/1.1149927

21. M. Otero-Leal, F. Rivadulla, S. S. Saxena, K. Ahilan, J. Rivas, Nature of the high-pressure tricritical point in MnSi. *Phys. Rev. B* **79**, 060401R (2009). doi:10.1103/PhysRevB.79.060401

22. M. Nomura, Y. Yamamoto, Y. Ochiai, H. Fujiwara, The measurement of the resistance of manganin wire with the cubic-anvil type pressure apparatus. *Jpn. J. Appl. Phys.* **18**, 363–366 (1979). doi:10.1143/JJAP.18.363

23. M. J. Frisch *et al*., Gaussian 09 (2010**)**.

24. C. Lee, W. Yang, R. G. Parr, Development of the Colle-Salvetti correlation-energy formula into a functional of the electron density. *Phys. Rev. B* **37**, 785–789 (1988). doi:10.1103/PhysRevB.37.785

25. B. Miehlich, A. Savin, H. Stoll, H. Preuss, Results obtained with the correlation energy density functionals of becke and Lee, Yang and Parr. *Chem. Phys. Lett.* **157**, 200–206 (1989). doi:10.1016/0009-2614(89)87234-3

26. T. A. Keith, R. F. W. Bader, Calculation of magnetic response properties using atoms in molecules. *Chem. Phys. Lett.* **194**, 1–8 (1992). doi:10.1016/0009-2614(92)85733-Q

27. T. A. Keith, R. F. W. Bader, Calculation of magnetic response properties using a continuous set of gauge transformations. *Chem. Phys. Lett.* **210**, 223–231 (1993). doi:10.1016/0009-2614(93)89127-4

28. J. R. Cheeseman, G. W. Trucks, T. A. Keith, M. J. Frisch, A comparison of models for calculating nuclear magnetic resonance shielding tensors. *J. Chem. Phys.* **104**, 5497–5509 (1996). doi:10.1063/1.471789